Enhancing Lunar Reconnaissance Orbiter Images via Multi-Frame Super Resolution for Future Robotic Space Missions

J. I. Delgado-Centeno, P. J. Sanchez-Cuevas, C. Martinez, and M.A. Olivares-Mendez

***Abstract*—This paper presents a novel application of a Multi-frame Super Resolution (MFSR) method for lunar surface imagery called *Lunar HighRes-net (L-HRN)*. In this work, we adapted and used NASA's Lunar Reconnaissance Orbiter (LRO) image database to train the Deep Learning architecture for image super resolution. Additionally, we also gathered an artificial image dataset from our virtual Moon to improve the amount of input data in the neural network training process. The network's architecture follows a standard MFSR algorithm that was enhanced for this specific use case. The proposed MFSR method has been evaluated using the well-known peak signal-to-noise ratio (PSNR) metric against other generic super-resolution methods of the state of the art. This work aims to improve environmental knowledge about the lunar surface to enhance future autonomous robots capabilities on the surface of the Moon.**

***Index Terms*—Space robotics and automation: aerial and field robotics.**

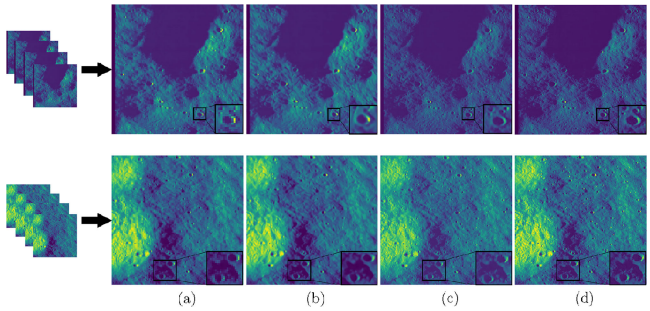

Fig. 1. Super resolution methods applied to NASA's LRO mission lunar surface images. (a) Bicubic, (b) ESDR, (c) Lunar HighRes-net (this work), and (d) Ground Truth. The images are presented in color map to perceive better the difference between the results of each super resolution method.

I. Introduction

SPACE applications are currently attracting the interest of several agencies and companies such as NASA, ESA, SpaceX and Blue Origin. They are investing a lot of resources in new missions [1]–[4] and exploitation plans. These missions present a wide variety of objectives and challenges, such as the study of the geological composition of celestial bodies and the study of life's presence at some point in the history of Mars, among others. In most cases, they involve robotic systems to perform *in-situ* and remote-sensing operations to avoid putting at risk human life or integrity. Two recent examples are the *Perseverance* rover [5] for Mars exploration and the *Volatile Investigating Polar Exploration Rover (VIPER)* [6] which will operate on the lunar surface. Particularly, *Perseverance* rover [5], has a crucial role in the NASA's Mars 2020 mission [2]. It counts with a wide variety of sensors to monitor and study the red planet's environmental conditions, evaluate signs of life and gather data to prepare human exploration in Mars. The *VIPER* rover [6] will explore the South Pole of the Moon and gather data about water-ice concentration in this region.

Nowadays, autonomous space missions heavily rely on the perception of the local environment. Moreover, it is well known that the conditions where rovers navigate are varied and harsh, and the success of the mission is ligated to have solid prior planning. Then, it is crucial to have a good understanding of the issues that a rover can face while performing its mission, such as the type of obstacles, slopes, and craters in the way of the robot.

In this sense, it is clear that having good models of the surface becomes necessary to select the landing site and optimally pre-plan the mission. This is a crucial part while defining a mission because, although the robot has onboard sensors to avoid dealing with unexpected situations, the chances of success are doubtful. Moreover, considering the limited endurance of these rovers due to extreme environmental conditions, it is vital to minimize this kind of reactivity actions. Fig 1 shows one specific result of this work applying image super resolution (SR) to lunar images. The authors identify this technique as a promising tool that can improve decision-making in future missions.

Pre-landing information is mostly obtained through remote sensing missions like NASA's Lunar Reconnaissance Orbiter (LRO) [7] and ISRO's Chandrayaan-2 [8]. The first one is a mission with the sole purpose of mapping the lunar surface by using satellite instrumentation, providing an almost complete lunar map. In contrast, the second one is a lunar exploration mission consisting of a lunar orbiter, a lander and a rover. In this

Manuscript received February 24, 2021; accepted June 20, 2021. Date of publication July 16, 2021; date of current version August 17, 2021. This letter was recommended for publication by Associate Editor J. Cacace and Editor P. Pounds upon evaluation of the reviewers' comments. *(Corresponding author: José Ignacio Delgado-Centeno.)*

The authors are with the SpaceR, Space Robotics Research Group, SnT Interdisciplinary Centre for Security, Reliability and Trust, University of Luxembourg, Luxembourg 1855, Luxembourg (e-mail: Jose.delgado@uni.lu; psanchez16@us.es; carol.martinezluna@uni.lu; miguel.olivaresmendez@uni.lu).

Digital Object Identifier 10.1109/LRA.2021.3097510

case, the orbiter analyzed the surface area prior to landing the rest of the mission's components with a high-resolution camera.

However, there can be complications due to the lack of resolution in the gathered data used with this purpose because it can potentially omit relevant details that would be vital for the mission's design. For example, NASA's LRO [7] have a resolution of up to 0.5 meters per pixel in the images obtained through the Narrow-Angle Camera (NAC). Furthermore, database statistics show that only a 40 % of the images are this accurate. The rest of the database presents half or worse (1-5 m/px) resolution, which could lead to the issues previously mentioned. Unfortunately, nowadays, the only alternative to improve this data seems to be the launch of new space missions with better instrumentation and sensors, which is costly and challenging to accomplish.

Image enhancement research on the field of remote sensing applied to space bodies has not been widely explored, but in its equivalent used on Earth imagery, there have been some improvements in recent years. In [10], [11] and [12] different methods of Single Image Super-Resolution (SISR) has been proved and applied to already existing databases. This SISR process enhances the quality of an image using either traditional Computer Vision (CV) algorithms or Deep Learning (DL) architecture, such as Convolutional Neural Networks (CNN) or Generative Adversarial Networks (GAN). Depending on the type of input image (RGB, Grayscale, Multispectral), the network varies, but the algorithms follow similar architectures. The improvement in the data quality can be obtained without any new mission and in a much faster manner. It is, therefore, a profitable and useful technique to be used in space robotics applications. As an alternative to SISR, another method can be used to achieve SR using multiple frames from the same image. This method is called Multi-Frame Super Resolution (MFSR), and it fuses the information available in each low resolution frame of a scene to generate a super resolution image. In [18], an example of this method applied to remote sensing is presented. A deep neural network is trained to perform the low-to-high resolution mapping from several remote sensing captures of the same image.

This work[1] aims to solve the lack of image quality problem by using the DL architecture *Lunar HighRes-net*. This network is based on the MFSR architecture of *HighRes-net* [13] and it has been applied to the data collected through NASA's LRO mission. The selection of this methodology was based on the study of its equivalent on Earth [10]–[12] that shows that this type of solutions provides a viable alternative to the launch on new and costly missions. Due to the importance of precision, while performing path planning for the missions, a multi-frame fusion method is employed instead of a single image one. The use of single captures of a particular region can lead to missing details as environmental conditions are decisive when gathering the information. The position of the sun, for example, can lead to shadow a region with rocks or smaller craters that won't appear in the image, potentially causing problems when navigating these areas during the mission. However, the use of multi-frame captures of a specific area of the surface will provide more details that will be taken into account while performing SR, as the images won't be captured under the same conditions.

The rest of the paper is structured as follows: Section II presents the different databases created for this work, including the source and the method used to obtain image datasets suited for the neural network training. Section III describes *Lunar HighRes-net*, the network architecture employed for the lunar surface MFSR. In Section IV, the results of this work are shown, both images and the metric used for the evaluation of the performance of the network. Lastly, in Section V the conclusions of this work are stated, and future lines of work are presented.

II. Moon's Surface Images

A. NASA's Lunar Reconnaissance Orbiter

NASA's LRO [7] mission started in 2009 with the objective of mapping the Moon to properly plan future space missions, providing information about craters, landing sites and regions of interest. Two stereo Narrow-Angle Cameras (NAC) and a Wide Angle Camera (WAC) performed remote sensing, capturing images of every sector of the Moon and providing three-dimensional information of the lunar surface thanks to the stereo image pair. After several years of orbiting the Moon, the mission was able to almost complete (98.2%) the map of the whole lunar surface. The regions that remain unmapped are mostly permanently shadowed areas within deep craters.

B. SpaceR's Virtual Moon

In the computer vision field, synthetic datasets have been becoming popular in the last few years. Artificial image datasets present an alternative to complete image collections for the training of neural networks. In both [23] [24], examples of the use of Unreal engine for the creation of virtual worlds and training scenarios are presented. In fields such as space, real images are hard to obtain, as the instrumentation used for this purpose is not easily accessible, and artificial datasets allow to have well-rounded databases. In [25], a virtual environment with lunar rocks was developed. This dataset presents an image collection suited for lunar surface image segmentation. Another example of these types of space synthetic data collection is introduced in [26], where a photorealistic simulator was created to train deep learning solutions for in orbit spacecraft pose estimation.

In order to improve the amount of data that would be used to train the SR neural network, we created an extra collection of images generated from a virtual model of the Moon designed using the graphic engine *Unreal Engine 4* [19]. As the software provides several tools for the alteration of the environment, the surface of the Virtual Moon can be modified as needed. They allow the possibility of adding and removing details to the scene whenever it is needed, which allows obtaining a complete and well-balanced details-wise dataset. Also, in *Unreal Engine 4* aerial images can be taken from the virtual lunar surface with different resolutions emulating a space remote sensing mission. Therefore, it can be used as ground truth to evaluate how the MFSR approach works. Some examples of both SpaceR's

[1]A video with a summary of our work was published in: https://youtu.be/3SA7qDRDJxU

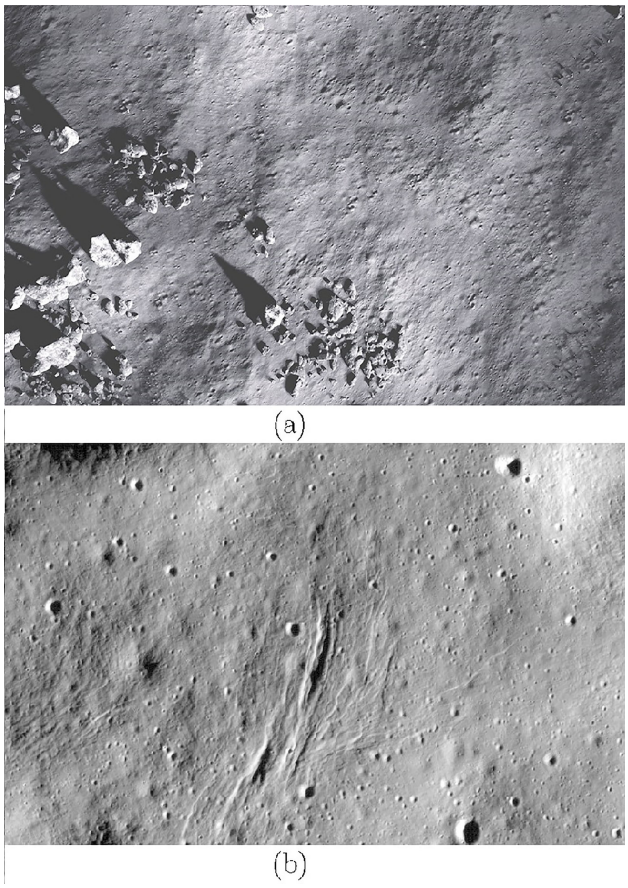

Fig. 2. Examples of the images used to generate the datasets of this work. (a) SpaceR's Virtual Moon, (b) NASA's LRO.

Virtual Moon and NASA's LRO images are shown in Fig. 2. Additionally, a diagram of the database creation process done for this work can be seen in Fig. 3. For the creation of the synthetic image dataset, a script was developed to emulate the flight of a satellite taking captures of the Virtual Moon's surface. After obtaining 100 images, the illumination conditions were changed and the script was launched again. This process was repeated four times and every gathered image was then downgraded and sliced to obtain the required patches and LR-HR sets for the training of the neural network.

C. Esa's Proba-V

The datasets used in this work follow the structure of the one used in [13], where an MFSR was developed to enhance the satellite images of the Earth of ESA's PROBA-V database [14]. PROBA-V was obtained by taking captures of the Earth's surface with an orbiting satellite. To every region of interest present in the dataset correspond at least 9 low resolution and one high resolution images. During this mission, a satellite captured low resolution (300 m/px) and high resolution (100 m/px) images from the surface of the Earth. Thus, each region captured in the database has one high and several low resolution images of the area due to the capture frequency set for the on-board sensors. Those images are also accompanied by metadata which provides

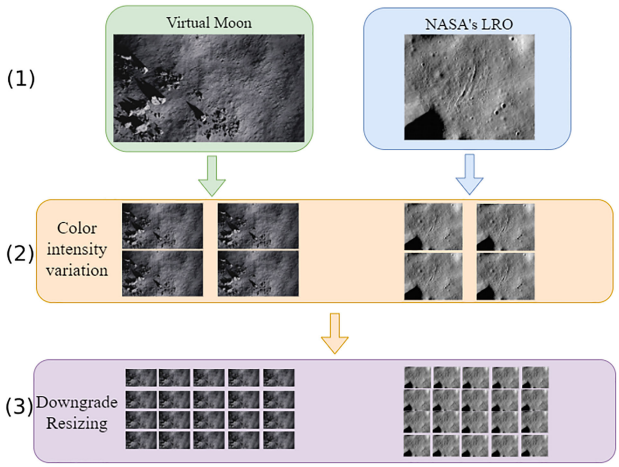

Fig. 3. Database creation diagram. The process can be described as: 1. Image acquisition (from LRO database and direct captures from the Virtual Moon), 2. color intensity variation to emulate different lighting conditions and 3. different downgrade methods applied for the resizing to obtain LR image sets for each scene.

much more details of every region, as the atmospheric and environmental conditions in which the low resolution images are taken are different.

The images from ESA's PROBA-V missions were taken from 74 different regions of the Earth at different points in time by the satellites of the said mission. The database is comprised of 1450 scenes, which are split into 1160 scenes for training and 290 scenes for testing. Each scene is represented by one grayscale HR image, with a 100 meters per pixel resolution and 9 to 20 grayscale LR images, with a resolution of 300 meters per pixel. The size of the images is 384×384 pixels for the HR ones and 128×128 pixels for the rest. Also, each image has associated a clearance map that indicates the area of the image that should not be processed by the neural network, as it is covered by clouds.

D. Datasets Adaptation

In this work, we prepared an equivalent to ESA's PROBA-V dataset using NASA's LRO and Virtual Moon images [2] for MFSR. In the case of the Virtual Moon, the illumination settings of the environment where modified to obtain 5 captures of the same scene with different illumination. In the case of LRO's images, the intensity of the pixel was modified to simulate the illumination change. Then, the same procedure was followed for both types of images. First, the original images were sliced in patches of 384x384 pixels, the considered ground truth. Then, the high resolution images were downscaled to generate low resolution (128×128 pixels) versions of them. By applying different interpolation methods, such as bicubic, bilinear and nearest neighbour, among others, every region of the lunar surface captured selected for the training of the network would have a ground truth and 20 low resolution images. This downgrade process allowed to perform MFSR on both lunar surface dataset.

[2]Both of the datasets utilized in this work are published and available to the public in: https://wwwfr.uni.lu/snt/research/spacer/datasets_tools, in their respective sections *LRO datasets* and *VirtualMoon.*

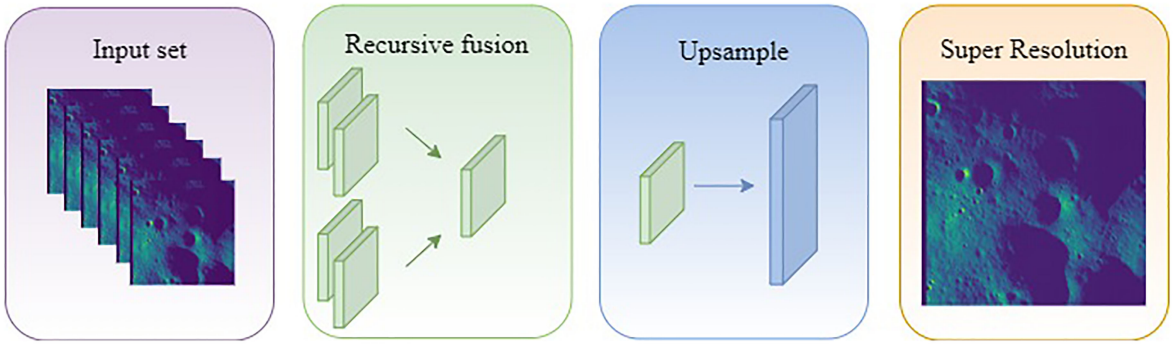

Fig. 4. Lunar HighRes-net MFSR diagram adapted from [13]. A set of multiple images of the same scenes are used as input of the network. These images are fused recursively in pairs in the embedding layer of the network. Finally, upsampling is performed and the SR image is generated.

Following the structure from ESA's PROBA-V, the 147 sets of images gathered from the Virtual Moon and the 60 sets from NASA's LRO are comprised by one HR grayscale image with a size of 384 × 384 pixels and 20 artificially downgraded LR grayscale images with a size of 128 × 128 pixels. The sets are divided into 135 for training and 12 for testing for the Virtual Moon database, and 54 for training and 6 for testing for LRO's database. The artificial downgrade was done over the HR images to be able to compare the results of the neural network when enhancing the resolution of the images x3. This downgrade was done rescaling the images using traditional CV interpolations and varying the color intensity of the images by 1%. This process emulates capturing images from the surface of the Moon at different points in time and with a variety of boundary conditions.

III. MFSR Method

A. Lunar HighRes-Net

Image super resolution methods [15] enhance the resolution of a single or multiple images using either traditional CV algorithms or DL techniques. In other words, it increases the perceptual quality and the number of details and features that appear in one captured scene. Even though the most widespread technique is SISR, in some cases, MFSR presents a good alternative to enhancing images with a lesser amount of details in the scene, like for instance, space images such as lunar surface pictures. The main assumption of MFSR is that a set of several views collectively contain more details than any single image of the same scene. The work presented in this paper focuses on the utilization of MFSR with lunar surface satellite imagery, as the enhancement of the images will provide higher perceptual quality and resolution. The current satellite images of the lunar surface or, in general, any celestial body often present a lack of precision in details about the surface characteristics, and therefore it can lead to imprecise planning of the space mission.

The neural network presented in this paper, *Lunar HighRes-net* follows the same architecture of [13]. It introduces *Highres-net*, a model to apply MFSR to remote sensing images of Earth inside a single spectral band (grayscale). In general, the network follows an encoder-decoder architecture that can be trained by using multiple images from the same scene. The input sets consist of a ground truth image with several lower resolution versions of it. This type of architectures works by fusing the information available in the low resolution images of a scene. The embedding layer of the network consists of a convolutional layer followed by two PReLU activations. The embedded states are fused recursively in pairs, reducing by a half its number each time. The final fused state contains the information of every view, and it is encoded into a HR state. Finally, this state is decoded into the resulting SR image. *HighRes-net* is paired with another network called *Shift-net* that would perform sub-pixel translations in order to align the ground truth and the super-resolution generated image. This operation ends up maximizing their similarities thanks to the sub-pixels shifts, thereby improving the quality of the results of the image enhancement. Fig. 4 shows the Lunar HighRes-Net architecture diagram of the process using the proposed network for MFSR.

The architecture of *HighRes-net* [13] included a clearance map to train the network to prevent clouds for interfering with the process. Thus, the network's recursive fusion layers would consider the clouds as a region with no information, while obtaining features and details from any of the others low-resolution captures of the same scene. In this work, we have modified this network architecture to avoid having this clearance map in the process and maximize how the dataset is exploited. Apart from this variation, *Lunar HighRes-net* follows the same pipeline. The input and output images of the network are 128 × 128 and 384 × 384 pixels respectively. Thus, the network perform a three times resolution scaling over the low resolution image set to produce the SR image. The datasets employed in the training and testing task have followed the same structure as the one used ESA's PROBA-V database originally, as it was stated in Section II.

B. Validation Metric - PSNR

For the evaluation of this work, the metric Peak Signal-to-Noise Ratio (PSNR) was used. It is the most used metric for SR evaluation. It defines the ratio between the maximum power of a signal and the noise that affects the fidelity of its representation. When applied to images, it can be easily defined via the Mean Squared Error (MSE). It can be described also as an objective metric to measure the quality of the reconstruction of a lossy

transformation. Given a monochrome image I and its noisy approximation N, the PSNR can be stated as:

$$MSE = \frac{1}{mn}\sum_{i=0}^{m-1}\sum_{j=0}^{n-1}[I(i,j) - N(i,j)]^2 \quad (1)$$

$$PSNR = 20 \cdot log_{10}(MAX_I) - 10 \cdot log_{10}(MSE) \quad (2)$$

where i and j are pixel's coordinates and MAX the maximum intensity pixel value of the image I.

This metric has been widely used in the state of the art for SR for a long time. In most cases, the average dB values of PSNR obtained by the latest research works are in the range 30-40 dB.

IV. Results

In this section, we validate the usage of the *Lunar HighRes-net* neural network for obtaining SR images of the lunar surface. To evaluate the performance of the network, the widely used metric Peak Signal-to-Noise Ratio is used, following most of the SR works in the literature. Additionally, three different training input for the network are presented in the section to perform a comparison among them. Lastly, the results produced by the network are introduced along with a comparison to other commonly used image SR methods.

A. Training and Transfer Learning

The training of the network to achieve SR on lunar surface images was divided into two main steps. First, a base training was done with ESA's PROBA-V as input. Then, while having the weights of this base training, a transfer learning approach was used to prepare the network to work with lunar images. Three different trainings were done to test the performance of the network using different inputs. The different trainings done over the network are:

1) PROBA-V: ESA's database was the only one used as an input for the training. The result trained network is equivalent to the original *HighRes-net*.
2) PROBA-V + Virtual Moon: This case includes the previous training, while performing transfer learning and training the network with additional image datasets from the Virtual Moon database.
3) PROBA-V + Virtual Moon + LRO: Finally, this case includes transfer learning from the previous one as well with another training with the extra input from the adapted NASA's LRO database.

The core training of the network with PROBA-V's database was done over 400 epochs, with a batch size of 8. This size was selected to be able to perform the training on a *Nvidia's RTX 2080* graphic card. Default hyperparameters for the ADAM optimizer and the same learning rates showed in [13]. For the training after the transfer learning with both Virtual Moon and LRO's databases, 100 epochs were selected, keeping the batch size and hyperparameters equal to the first part of the training.

The average values of PSNR, in dB, obtained through the training with the three different inputs were analyzed to look for the best results for both Virtual Moon and LRO databases, concluding that the combination of the three presented datasets was key to a multipurpose solution for both image collections.

TABLE I
Average PSNR Training Results With Different Input Datasets (in dB)

Training input	Virtual Moon	LRO
PROBA-V	31	23
PROBA-V + VM	38	28
PROBA-V + VM + LRO	38	31

TABLE II
PSNR Values Comparison Between Different SR Methods (in dB)

Img	Bicubic	FSRCNN	ESPCN	ESDR	L-HRN
L01	23.89	24.28	24.25	24.29	31.61
L02	26.45	26.79	27.03	27.24	30.76
L03	25.08	25.63	25.60	25.91	28.11
L04	27.67	28.38	28.37	28.61	31.42
L05	26.02	26.69	26.68	27.21	28.98
V00	31.80	33.04	32.94	33.29	47.81
V01	26.53	27.84	27.94	28.15	39.81
V02	32.61	35.99	35.23	35.73	39.38
V03	26.51	27.05	27.16	27.19	39.11
V04	30.72	33.36	33.33	34.19	38.31
V05	29.32	32.48	32.48	33.01	41.88
V06	27.06	28.25	28.13	28.69	40.09
V07	31.06	34.08	34.20	35.41	41.98
V08	29.53	31.52	31.52	32.43	39.55
V09	32.31	35.23	35.26	36.34	43.53
V10	28.24	30.33	30.26	31.38	39.76
V11	26.75	27.40	27.35	27.55	36.72
Avg.	28.33	29.90	29.87	30.39	**37.58**

Lunar HighRes-net trained with images from the three databases presented in this work have been proven to provide the best results, as it can be seen in Table I. The addition of LRO's images to the training does not increase the SR performance of the network with Virtual Moon's images. However, it can be seen how the image enhancement of LRO does improve when including every type of dataset. It can also be seen how the *Lunar HighRes-net* network perform better with lunar surface images and a complete training than the base *HighRes-net*.

B. MFSR Results

For the experiments, the test image set defined previously in the databases was used. They consist of the comparison between the high resolution ground truth and the super resolution image generated using the presented network. *Lunar HighRes-net* has been evaluated using the images from both the Virtual Moon and NASA's LRO defined in Section II with the PSNR metric. These results have been compared with other SR techniques to validate that *Lunar HighRes-net* is a valid approach to lunar surface image enhancement, and it achieves state of the art scores. The results of enhancing the input dataset resolution x3 with the different solutions are presented in the Table II. We used the well-known open-source computer vision library *OpenCV* as it has built-in methods that use networks for image SR that were evaluated in lunar imagery for reference. For the comparison, image scaling with bicubic interpolation was used to have a reference of a SR traditional computer vision method. Additionally, three machine learning methods were used: *EDSR* [20], *ESPCN* [21] and *FSRCNN* [22]. These networks have been

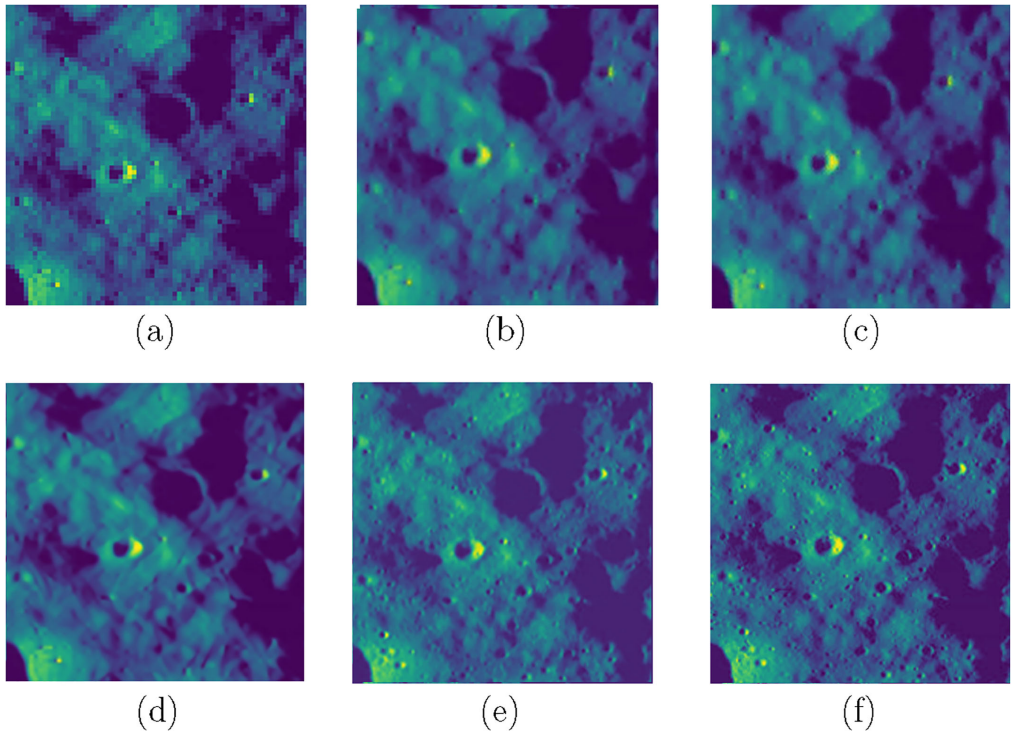

Fig. 5. Full image comparison between the different SR methods used in this paper. (a) Bicubic, (b) ESPCN, (c) FSRCNN, (d) EDSR, (e) Lunar HighRes-net, (f) Ground truth. The size of the figure makes it possible to better appreciate the difference between methods.

proved to provide high detailed SR image solutions for many applications, such as botanic and zoological imagery. Due to the wide variety of SR applications where these architectures can be utilized, they were selected for the comparison in this work. These implementations were used on the lunar surface imagery, and the results were evaluated comparing the SR version of the scene with the ground truth also with the PSNR metric. Fig. 5 presents an example of the results obtained with the different SR algorithms.

The quality of the generated SR images compared with the ground truth of the test dataset is evaluated with the PSNR metric in Table II. The results obtained after performing SR on lunar images from both LRO and the Virtual Moon datasets with the different methods are displayed. Bicubic interpolation is one of the most basic traditional computer vision algorithms of resolution enhancement, and it is compared as reference with the rest of the methods. FSRCNN [22], ESPCN [21] and EDSR [20] are selected as generic methods of deep learning SR for comparison. Finally, the Lunar HighRes-net column shows the results of this work, after the training with the combined remote sensing datasets previously mentioned. The results of Table II show that *Lunar HighRes-net* provides the best results according to the PSNR when compared to the other methods. Furthermore, a perceptual quality increase can be seen in the output of the network. Some examples of the output of the network can be seen in Fig 6 along with one of the input images and the ground truth. High level features present in these images, such as rocks or craters, show the easiest to notice resolution enhancement achieved with *Lunar HighRes-net*. Even though

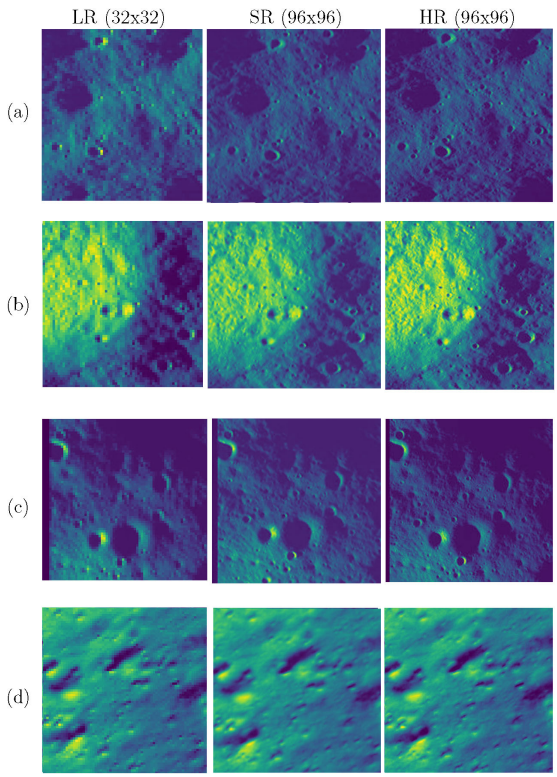

Fig. 6. Results from using Lunar HighRes-net on different images of the databases created for this work. (a), (b), (c) LRO images, (d) Virtual Moon image. The following link provides a folder with real size images: https://wwwfr.uni.lu/snt/research/spacer/datasets_tools, in the corresponding section of *Lunar High-ResNet results.*

some of the SR images from the Virtual Moon display a high PSNR due to the presence of small shadowed regions in the scene, it can also be seen that the results of the x3 enhancement achieve similar results to other SR network architectures in the field of image improvement. As it was mentioned the average values obtained in the process are similar to the state of the art in image SR.

V. Conclusion

In this work, we presented *Lunar HighRes-net*, a deep-learning based Multi-Frame Super Resolution method to enhance images of the Moon's surface. We also introduced and shared two databases that have been created for the training of the presented network, one adapted from NASA's Lunar Reconnaissance Orbiter mission imagery and a second one obtained from a virtual Moon developed in *Unreal Engine 4*. These databases are composed of image sets both artificial and real of lunar surface images. Each set contains one high resolution image (384×384 pixels) and 20 corresponding low resolution images (128×128 pixels) of the same scene. A transfer learning approach was performed from ESA's PROBA-V database training. Training results evidence that the addition of the new datasets created for this work to the training process of the network improve the performance of the network. The results obtained with *Lunar HighRes-net* achieves state of the art performance (35-40 dB) according to the results evaluated with the well-known Peak Signal-to-Noise Ratio for both image datasets. It also presents a significant quality improvement over other well known deep learning super-resolution approaches. Future work in this research line will focus on fine-tuning performed over the network *Lunar HighRes-net*. Additionally, new deep-learning architectures based on Generative Adversarial Networks (GAN) will be explored for space images super-resolution. These type of networks achieve better results in some cases of the state of the art of super-resolution when compared with convolutional architectures. Lastly, it will be studied the estimation of 3-dimensional information from super-resolution stereo image pairs. This will allow to increase the precision of the elevation maps of the lunar surface and therefore aid in preparing new space robotic missions on the Moon.

References

[1] M. Smith *et al.*, "The artemis program: An overview of NASA's activities to return humans to the Moon," in *Proc. IEEE Aerosp. Conf.*, Big Sky, MT, USA, 2020, pp. 1–10.

[2] K. H. Williford *et al.*, "The NASA Mars 2020 rover mission and the search for extraterrestrial life," *From Habitability Life Mars*, Elsevier, 2018, pp. 275–308.

[3] J. Vago *et al.*, "ESA ExoMars program: The next step in exploring Mars." *Sol. System Res.*, vol. 49, no. 7, 2015, pp. 518–528.

[4] T. Hoshino *et al.*, "Lunar polar exploration mission for water prospection-JAXA's current status of joint study with ISRO," *Acta Astronautica*, vol. 176, pp. 52–58, 2020.

[5] J. N. Maki *et al.*, "The mars 2020 engineering cameras and microphone on the perseverance rover: A next-generation imaging system for mars exploration," *Space Sci. Rev.* vol. 216, no. 8, pp. 1–48, 2020.

[6] A. Colaprete *et al.*, "An overview of the volatiles investigating polar exploration rover (VIPER) mission," in *Proc. AGU Fall Meeting Abstr.*, 2019, pp. P34B–03.

[7] G. Chin *et al.*, "Lunar reconnaissance orbiter overview: Theáinstrument suite and mission," *Space Sci. Rev.*, vol. 129, no. 4, pp. 391–419, 2007.

[8] J. N. Goswami, and M. Annadurai, "Chandrayaan-2 mission," in *Proc. Lunar Planet. Sci. Conf.*, no. 1608, p. 2042, 2011.

[9] R. W. Zurek, and S. E. Smrekar, "An overview of the Mars reconnaissance orbiter (MRO) science mission," *J. Geophysical Res.: Planets*, vol. 112, no. E5, 2007.

[10] J. M. Haut, R. Fernandez-Beltran, M. E. Paoletti, J. Plaza, and A. Plaza, "Remote sensing image superresolution using deep residual channel attention," *IEEE Trans. Geosci. Remote Sens.*, vol. 57, no. 11, pp. 9277–9289, Nov. 2019.

[11] K. Jiang, Z. Wang, P. Yi, J. Jiang, J. Xiao, and Y. Yao, "Deep distillation recursive network for remote sensing imagery super-resolution," *Remote Sens.*, vol. 10, no. 11, p. 1700, 2018.

[12] Y. Zhang *et al.*, "Pqa-cnn: Towards perceptual quality assured single-image super-resolution in remote sensing," in *Proc. IEEE/ACM 28th Int. Symp. Qual. Serv.*, 2020, pp. 1–10.

[13] M. Deudon *et al.*, "HighRes-Net: Recursive fusion for multi-frame super-resolution of satellite imagery," 2020, *arXiv:2002.06460*.

[14] M. Francois, S. Santandrea, K. Mellab, D. Vrancken, and J. Versluys, "The PROBA-V mission: The space segment," *Int. J. Remote Sens.*, vol. 35, no. 7, pp. 2548–2564, 2014.

[15] S. C. Park, M. K. Park and M. G. Kang, "Super-resolution image reconstruction: A technical overview," *IEEE Signal Process. Mag.*, vol. 20, no. 3, pp. 21–36, May 2003.

[16] H. Greenspan, "Super-resolution in medical imaging," *Comput. J.*, vol. 52, no. 1, pp. 43–63, 2009.

[17] R. Fernandez-Beltran, P. Latorre-Carmona and F. Pla, "Single-frame super-resolution in remote sensing: A practical overview," *Int. J. Remote Sens.*, vol. 38, no. 1, pp. 314–354, 2017.

[18] M. Kawulok, P. Benecki, S. Piechaczek, K. Hrynczenko, D. Kostrzewa and J. Nalepa, "Deep learning for multiple-image super-resolution," *IEEE Geosci. Remote Sens. Lett.*, 17, no. 6, pp. 1062–1066, Jun. 2020.

[19] Unreal Engine 4, [Online]. Available: https://www.unrealengine.com/

[20] B. Lim, S. Son, H. Kim, S. Nah and K. M. Lee, "Enhanced deep residual networks for single image super-resolution," in *Proc. IEEE Conf. Comput. Vis. Pattern Recognit. Workshops*, 2017, pp. 136–144.

[21] W. Shi *et al.*, "Real-time single image and video super-resolution using an efficient sub-pixel convolutional neural network," in *Proc. IEEE Conf. Comput. Vis. Pattern Recognit.*, 2016, pp. 1874–1883.

[22] C. Dong, C. C. Loy, and X. Tang, "Accelerating the super-resolution convolutional neural network," in *Proc. Eur. Conf. Comput. Vis.*, 2016, pp. 391–407.

[23] W. Qiu *et al.*, "Unrealcv: Virtual worlds for computer vision," in *Proc. 25th ACM Int. Conf. Multimedia*, 2017, pp. 1221–1224.

[24] A. Garcia-Garcia *et al.*, "The robotrix: An extremely photorealistic and very-large-scale indoor dataset of sequences with robot trajectories and interactions," in *Proc. IEEE/RSJ Int. Conf. Intell. Robots Syst.*, 2018, pp. 6790–6797.

[25] R. Pessia and G. Ishigami, "Artificial Lunar Landscape Dataset," [Online]. Available: https://www.kaggle.com/romainpessia/artificial-lunar-rocky-landscape-dataset

[26] P. F. Proença and Y. Gao, "Deep learning for spacecraft pose estimation from photorealistic rendering," in *Proc. IEEE Int. Conf. Robot. Automat.*, 2020, pp. 6007–6013.